Interference and Noise Cancellation Based on Complex/Real-Valued Blind Maximum-A-Posteriori Probability Algorithms with Symmetric Constraint

Jiunn-Yann Chen[#], Yao-Jen Chang[*], Chia-Lu Ho[#]

[#]*Department of* Communication *Engineering, National Central University, Chungli, Taiwan*
[*]*Industrial Technology Research Institute, Chutung, Taiwan*

[#]*100523019@cc.ncu.edu.tw,* [*]*britpablo@itri.org.tw,* [#]*aluglory@ncu.edu.tw*

***Abstract*—In this paper, we propose a complex-valued symmetry-constrained maximum-a-posterior probability (SC-MAP) algorithm and a real-valued SC-MAP (RSC-MAP) algorithm for concurrent adaptive filter (CAF) applied to beamforming. We first contribute to deriving a closed-form optimal weight expression for blind MAP algorithm. A conjugate symmetric property associated with optimal blind MAP weights is further acquired. Then, we use the conjugate symmetric constraint to guide the proposed SC-MAP and RSC-MAP algorithms to follow the optimal blind MAP expression form during adapting procedure. In the simulations, we show that the proposed SC-MAP and RSC-MAP algorithms have better performance than the classic ones. Compared with SC-MAP, the RSC-MAP with less computational complexity has the same bit-error rate performance.**

***Keywords*—Maximum-a-posteriori probability estimation (MAP), constant modulus algorithm (CMA), beamforming, filtering.**

1. INTRODUCTION

Adaptive filter applied to beamformer can receive the desired signals while suppressing the interfering ones. There have been various applications to antenna array and communications [1-8]. The reference-based algorithms [1-7] can effectively adapt the weights of filter, but the required reference data would reduce the system throughput. The blind algorithms [1-2, 8-18], like constant modulus algorithm (CMA), have higher throughput by avoiding the use of reference data. However, decision ambiguity often occurs in blind algorithms.

Recently, experts [9-17] developed a concurrent adaptive filter (CAF), which can concurrently employ two kinds of blind algorithms and acquire better performance than classic adaptive filters. The concurrent CMA and decision directed algorithm (CMA+DD) [9-11] was first studied for CAF. The CMA+DD with a complexity that is more than twice of CMA can alleviate the decision ambiguity. The concurrent CMA and maximum a-posteriori probability algorithm (CMA+MAP) was studied in various scenarios [12-17]. With less complexity, CMA+MAP has a similar steady-state performance to CMA+DD. However, a slow-converging problem still makes blind algorithms impractical in many real-time applications.

The MAP method actually has been employed in both reference-based [4,5] and blind algorithms [12-18]. None of these works discusses a closed-form solution for MAP. In this paper, a derived conjugate symmetry of optimal MAP expression is given. To the best of our knowledge, no past research papers have investigated on a symmetry-constrained for the blind MAP algorithm. Based on this conjugate symmetry property of blind MAP, we propose a concurrent CMA and complex-valued symmetry-constrained MAP algorithm (CMA+SC-MAP). Subsequently, we further propose a concurrent CMA and real-valued SC-MAP algorithm (CMA+RSC-MAP) based on two real-valued update equations to independently update the filter weights. Under this manner, CMA+RSC-MAP can obtain less computational complexity than CMA+SC-MAP. We will show in simulations that CMA+SC-MAP and CMA+RSC-MAP are superior to the classic algorithms in terms of bit-error rate (BER) and signal constellation.

2. SYSTEM MODEL

The model studied is a uniform linear array with M sensors. The adjacent space d_a between sensors is less than half of signal wavelength λ_a to avoid aliasing. Suppose there are L narrowband and uncorrelated signals impinging on the array with different directions of angles (DOA) $\theta_0,...,\theta_{L-1}$, respectively. The received array signals at the nth snapshot are expressed as [6-8]

$$\boldsymbol{x}(n) \equiv [x_0(n),...,x_{M-1}(n)]^T = \boldsymbol{A}\cdot\boldsymbol{s}(n)+\boldsymbol{n}(n), \quad (1)$$

Where $s(n) \equiv [s_0(n),...,s_{L-1}(n)]^T$ are source signals, $\boldsymbol{n}(n)$ is the white noise vector with $E[\boldsymbol{n}(n)\boldsymbol{n}^H(n)] = 2\sigma_n^2\boldsymbol{I}_M$, $\boldsymbol{A} \equiv [\boldsymbol{a}(\psi_0),\boldsymbol{a}(\psi_1),...,\boldsymbol{a}(\psi_{L-1})]$ is a mixing matrix and $\boldsymbol{a}(\psi_l) \equiv [1,e^{-j\psi l},...,e^{-j(M-1)\psi l}]^T$ is the array steering vector with $\psi_l = 2\pi d_a \sin(\theta_l)/\lambda_a$[1−8]. By using a set of filter weights $\boldsymbol{w} \equiv [w_0,...,w_{M-1}]^T$, the filter output is $y(n) = \boldsymbol{w}^H\boldsymbol{x}(n)$.

3. THE PROPOSED BLIND ALGORITHM

3.1. Optimal Weight Expression of Blind MAP Algorithm

A closed-form optimal weight expression for blind MAP algorithm is derived here. Without loss of generality, we assume that the desired signal $s_d(n)$ is related to the first element of $s(n)$. When the weight vector $\boldsymbol{w}$ has been optimally chosen in the steady state, the filter output can be expressed as

$$y(n) \approx s_d(n) + v(n), \quad (2)$$

where $s_d(n)$ is chosen from one of the elements in the N^2-QAM symbol set:

$$S \equiv \left\{ s_{iq} \middle| s_{iq} \equiv \frac{2i-N-1}{F} + j\frac{2q-N-1}{F},\ 1 \le i,q \le N \right\}, \quad (3)$$

Where N is the bit number of each symbol, F is normalized factor to make $E[|s_d|^2]=1$ and $v(n)$ is approximate Gaussian distribution with zero mean and an variance of $2\sigma_n^2\boldsymbol{w}^H\boldsymbol{w}$. With equal probabilities of s_{iq}, an approximation of the a posteriori pdf of $y(n)$ can be modeled by N^2 Gaussian clusters with means s_{iq} and a variance ρ related to $\sigma_n^2\boldsymbol{w}^H\boldsymbol{w}$:

$$\hat{p}(\boldsymbol{w},y(n)) \approx \sum_{i,q}\frac{1}{2N^2\pi\rho}e^{-\frac{|y(n)-s_{iq}|^2}{2\rho}}. \quad (4)$$

We derive the optimal weight expression of the blind MAP algorithm by maximizing the mean value of $\hat{p}(\boldsymbol{w},y(n))$:

$$\max J_o(\boldsymbol{w}) = E[\hat{p}(\boldsymbol{w},y(n))]. \quad (5)$$

To find the maximum value, we use the gradient descent method, i.e., $\partial J_o(\boldsymbol{w})/\partial \boldsymbol{w}^* = 0$, to obtain the expression:

$$\sum_{i,q} E[e^{-\frac{|y(n)-s_{iq}|^2}{2\rho}}(\boldsymbol{x}(n)\boldsymbol{x}^H(n)\boldsymbol{w} - \boldsymbol{x}(n)s_{iq}^*)] = 0. \quad (6)$$

As the weights converge to the optimal solution in steady state, the output $y(n)$ should be geometrically near $s_d(n)$, and far away from the locations associated with $s_{iq} \ne s_d(n)$. If ρ is chosen properly, the values of the exponential functions related to $s_{iq} \ne s_d(n)$ in (6) would be very small. Thus the equation for the optimal blind MAP expression can be simplified as

$$E[e^{-\frac{|y(n)-\hat{s}_d|^2}{2\rho}}(\boldsymbol{x}(n)\boldsymbol{x}^H(n)\boldsymbol{w} - \boldsymbol{x}(n)\hat{s}_d^*)] = 0, \quad (7)$$

where $\hat{s}_d(n)$ is the blind MAP estimate of $s_d(n)$. Due to $y(n)$ geometrically located near $s_d(n)$ in steady-state as formulated in (2), $\hat{s}_d(n)$ should be also uncorrelated to $s_1(n),...,s_{L-1}$. Besides, the system model (1) can be rewritten as

$$\boldsymbol{x}(n) = \sum \boldsymbol{a}(\psi_i)s_i(n) + \boldsymbol{n}(n). \quad (8)$$

Accordingly, the optimal weight expression for blind MAP algorithm can be expressed as

$$\boldsymbol{w} = c\boldsymbol{R}^{-1}\boldsymbol{a}(\psi_0), \quad (9)$$

where $\boldsymbol{R} = E[\boldsymbol{x}(n)\boldsymbol{x}^H(n)]$ and $c \equiv E[s_0(n)\hat{s}_d^*(n)]$.

The derived optimal blind MAP expression (9) is very similar to the well-known reference-based sample matrix inversion (SMI) one [2], which is seen as an optimal solution of linear adaptive filter. Unfortunately, we cannot directly use the weight expression (9) to obtain the optimal blind MAP solution in reality, since c depends on $\hat{s}_d(n)$, which is a function of $\boldsymbol{w}$. However, we can extract a useful conjugate symmetric property from the optimal expression (9) to further design the proposed blind algorithm. This conjugate symmetric property is as follows:

$$\boldsymbol{w} = e^{j\phi_{MC}}\boldsymbol{J}\boldsymbol{w}^*, \quad (10)$$

where $\phi_{MC} = 2\phi_c - (M-1)\psi_0$, ϕ_c is the phase of c and the matrix $\boldsymbol{J}$ is defined as

$$\boldsymbol{J} = \begin{bmatrix} 0 & \cdots & 0 & 1 \\ 0 & \cdots & 1 & 0 \\ \vdots & \ddots & \vdots & \vdots \\ 1 & \cdots & 0 & 0 \end{bmatrix}. \tag{11}$$

Proof. Note that $\boldsymbol{JJ} = \boldsymbol{I}$, and $\boldsymbol{R}$ is a centro-Hermitian matrix. We have $\boldsymbol{R} = \boldsymbol{J}\boldsymbol{R}^*\boldsymbol{J}$ and $\boldsymbol{R}^{-1} = \boldsymbol{J}(\boldsymbol{R}^{-1})^*\boldsymbol{J}$. The steering vector has the property of $\boldsymbol{a}(\psi_0) = e^{-j(M-1)\psi_0}\boldsymbol{J}\boldsymbol{a}^*(\psi_0)$. The property of the optimal blind MAP expression is acquired as follows:

$$\begin{aligned} \boldsymbol{w} &= c\boldsymbol{R}^{-1}\boldsymbol{a}(\psi_0) \\ &= c\boldsymbol{J}(\boldsymbol{R}^{-1})^*\boldsymbol{J}e^{-j(M-1)\psi_0}\boldsymbol{J}\boldsymbol{a}^*(\psi_0) \\ &= \frac{c}{c^*}e^{-j(M-1)\psi_0}\boldsymbol{J}\boldsymbol{w}^* \\ &= e^{j[2\phi_c-(M-1)\psi_0]}\boldsymbol{J}\boldsymbol{w}^*. \end{aligned} \tag{12}$$

Next, we will show that this property provides a powerful constraint to design the proposed blind SC-MAP algorithm.

3.2. Concurrent CMA and SC-MAP algorithm

The blind CMA is known to be capable of opening an 'initially closed eye' for CAF [9-17]. However, the CAFs, such as CMA+DD and CMA+MAP, still require a large number of snapshots to achieve a satisfactory performance in many applications. We propose to add the optimal blind MAP property (10) into the proposed CMA+SC-MAP algorithm.

The weight vector of CMA+SC-MAP contains two parts:

$$\boldsymbol{w} = \boldsymbol{w}_c + \boldsymbol{w}_m, \tag{13}$$

where filter weights $\boldsymbol{w}_c$ and $\boldsymbol{w}_m$ are, respectively, for the CMA algorithm and the proposed SC-MAP algorithm. Based on the CMA cost rule with a constant $R \equiv E(|s_d(n)|^4)/E(|s_d(n)|^2)$:

$$\min J_c(\boldsymbol{w}) = \frac{1}{4}(|y(n)|^2 - R)^2, \tag{14}$$

the weights $\boldsymbol{w}_c$ is updated as

$$\boldsymbol{w}_c(n+1) = \boldsymbol{w}_c(n) + \mu_c(R - |y(n)|^2)y^*(n)\boldsymbol{x}(n), \tag{15}$$

where μ_c is the stepsize. The weights $\boldsymbol{w}_{\mathrm{m}}$ by contrast are updated based on the proposed SC-MAP. Because ϕ_{MC} in (10) is unknown to a blind algorithm, we decompose $\boldsymbol{w}_m$ as $\boldsymbol{w}_m = \alpha_m^*\boldsymbol{w}_{ms}$ to avoid the direct operation on ϕ_{MC}, where $\alpha_m = e^{-j\phi_{MC}/2}$ and $\boldsymbol{w}_{ms} = e^{-j\phi_{MC}/2}\boldsymbol{w}_m$. Note that $|\alpha_m| = 1$. Based on (10), it can be easily proved that the created weights $\boldsymbol{w}_{ms}$ also satisfy the conjugate symmetry:

$$\boldsymbol{w}_{ms} = \boldsymbol{J}\boldsymbol{w}_{ms}^*. \tag{16}$$

To derive the adaptive blind SC-MAP algorithm, the MAP rule (5) associated with the complex-valued filter output $y(n)$ is equivalently modified as an instantaneous log rule $J_m(\boldsymbol{w})$, and the symmetric constraint (16) is added to guide the weights $\boldsymbol{w}_m$ obeying the optimal blind MAP property:

$$\max J_m(\boldsymbol{w}_{ms}, \alpha_m) = \rho \log[\hat{p}(\boldsymbol{w}, y(n))] \quad \text{subject to } \boldsymbol{w}_{ms} = \boldsymbol{J}\boldsymbol{w}_{ms}^*. \tag{17}$$

To transform the constrained MAP rule into an unconstrained maximum problem (17) is modified as the following cost rule:

$$Q = J_m(\boldsymbol{w}_{ms}, \alpha_m) + \frac{\lambda(n)}{\|\boldsymbol{w}_{ms}(n) - \boldsymbol{J}\boldsymbol{w}_{ms}^*(n)\|^2}, \tag{18}$$

where the undetermined multiplier $\lambda(n)$ is a real number due to $\|\boldsymbol{w}_{ms}(n) - \boldsymbol{J}\boldsymbol{w}_{ms}^*(n)\|^2$ being a real value. We take the gradient of (18) with respect to $\boldsymbol{w}_{ms}^*$ and α_m, respectively, as

$$\nabla_{\boldsymbol{w}_{ms}^*} Q = \Delta_{\mathbf{m}}(n)\alpha_m(n)\boldsymbol{x}(n) - \frac{2\lambda(n)(\boldsymbol{w}_{ms}(n) - \boldsymbol{J}\boldsymbol{w}_{ms}^*(n))}{\|\boldsymbol{w}_{ms}(n) - \boldsymbol{J}\boldsymbol{w}_{ms}^*(n)\|^4} \tag{19}$$

and

$$\nabla_{\alpha_m} Q = \Delta_{\mathbf{m}}(n)\boldsymbol{w}_{ms}^H(n)\boldsymbol{x}(n), \tag{20}$$

where

$$\Delta_m(n) \equiv \frac{\sum_{i,q} \frac{1}{2N^2\pi\rho}\exp(-\frac{|y(n) - s_{iq}|^2}{2\rho})(s_{iq} - y(n))^*}{\hat{p}(\boldsymbol{w}, y(n))}. \tag{21}$$

The weight vector of SC-MAP is updated in the positive direction of the gradient (19), scaled by the stepsize μ_m:

$$\begin{aligned} \boldsymbol{w}_{ms}(n+1) = \boldsymbol{w}_{ms}(n) &+ \mu_m\Delta_{\mathbf{m}}(n)\alpha_m(n)\boldsymbol{x}(n) \\ &- \frac{2\mu_m\lambda(n)(\boldsymbol{w}_{ms}(n) - \boldsymbol{J}\boldsymbol{w}_{ms}^*(n))}{\|\boldsymbol{w}_{ms}(n) - \boldsymbol{J}\boldsymbol{w}_{ms}^*(n)\|^4}. \end{aligned} \tag{22}$$

Because $\boldsymbol{w}_{ms}(n+1)$ is constrained to obey the property of the optimal blind MAP expression, we substitute (22) into (16):

$$\frac{2\mu_m \lambda(n)(\boldsymbol{w}_{ms}(n) - \boldsymbol{J}\boldsymbol{w}_{ms}^*(n))}{\| \boldsymbol{w}_{ms}(n) - \boldsymbol{J}\boldsymbol{w}_{ms}^*(n)\|^4} = \frac{\mu_m}{2}(\boldsymbol{\Delta}(n) - \boldsymbol{J}\boldsymbol{\Delta}^*(n)), \tag{23}$$

where

$$\boldsymbol{\Delta}(n) \equiv \frac{\partial J_m(\boldsymbol{w}_{ms}, \alpha_m)}{\partial \boldsymbol{w}_{ms}^*} = \Delta_{\mathbf{m}}(n)\alpha_m(n)\boldsymbol{x}(n) \cdot \tag{24}$$

By substituting (23) into (22), we get the final updated $\boldsymbol{w}_{\mathrm{ms}}$:

$$\boldsymbol{w}_{ms}(n+1) = \boldsymbol{w}_{ms}(n) + \frac{\mu_m}{2}(\boldsymbol{\Delta}(n) + \boldsymbol{J}\boldsymbol{\Delta}^*(n)). \tag{25}$$

We also update α_m in the positive direction of the gradient (20), scaled by the stepsize μ_α, and make sure it is normalized:

$$\begin{cases} \hat{\alpha}_m(n+1) = \alpha_m(n) + \mu_\alpha \Delta_{\mathbf{m}}(n)\boldsymbol{w}_{ms}^H(n)\boldsymbol{x}(n) \\ \alpha_m(n+1) = \hat{\alpha}_m(n+1) / |\hat{\alpha}_m(n+1)|. \end{cases} \tag{26}$$

Then we get $\boldsymbol{w}_{\boldsymbol{m}}(n+1) = \alpha_m^*(n+1)\boldsymbol{w}_{ms}(n+1)$ containing the property of the optimal blind MAP weight expression.

By adding the constraint to the MAP cost rule, the algorithm structure of the proposed CMA+SC-MAP is very different from that of the traditional ones and gives an alternate choice for further designs. The choice of ρ should be small enough to prevent breaking the assumption of (7). Because α_m influences the phase of $\boldsymbol{w}_m$ only, μ_α is not sensitive to the performance.

3.3. Concurrent CMA and RSC-MAP algorithm

Although CMA+SC-MAP algorithm would acquire bit-error rate (BER) performance close to optimal solutions in a few adaptations, a low-complexity version of CMA+SC-MAP is preferred. By splitting the complex-valued derivation in Section 3.2 into two independent real-valued derivations, a real-valued SC-MAP (RSC-MAP) algorithm is proposed in this sub-section.

In the following, the $\{\cdot\}_{\mathrm{R}}$ and $\{\cdot\}_{\mathrm{I}}$ donate the real part and the imaginary part of the complex number vector. The SC-MAP weights $\boldsymbol{w}_{\mathrm{ms}}$ satisfy the conjugate symmetry $\boldsymbol{w}_{ms} = \boldsymbol{J}\boldsymbol{w}_{ms}^*$, but RSC-MAP algorithm split this single-symmetry into two real-valued symmetries:

$$\boldsymbol{w}_{msR} = \boldsymbol{J}\boldsymbol{w}_{msR}, \tag{27}$$

and

$$\boldsymbol{w}_{msI} = -\boldsymbol{J}\boldsymbol{w}_{msI}, \tag{28}$$

Similar to CMA+SC-MAP, the CMA+RSC-MAP weight vector contains two pairs:

$$\begin{aligned} \boldsymbol{w} &= \boldsymbol{w}_c + \boldsymbol{w}_m \\ &= (\boldsymbol{w}_{cR} + \boldsymbol{w}_{mR}) + j(\boldsymbol{w}_{cI} + \boldsymbol{w}_{mI}) \end{aligned}. \tag{29}$$

We also get the filter output as

$$y = (\boldsymbol{w}_R^T \boldsymbol{x}_R + \boldsymbol{w}_I^T \boldsymbol{x}_I) + j(\boldsymbol{w}_R^T \boldsymbol{x}_I - \boldsymbol{w}_I^T \boldsymbol{x}_R), \tag{30}$$

Differing from cost rule (17) associated complex-valued y_R, we consider the MAP cost rules associated with real-valued $y_R(n)$ and $y_I(n)$ and constrain them to follow the real-valued symmetries (27-28), respectively:

$$\max J_{mR}(\boldsymbol{w}_{ms}, \alpha_m) = \rho log\left[\hat{p}_R \equiv \sum_i \frac{1}{2\sqrt{2\pi\rho}} exp(-\frac{(y_R - s_i)^2}{2\rho})\right],$$

subject to $\boldsymbol{w}_{msR} = \boldsymbol{J}\boldsymbol{w}_{msR}$ (31)

and

$$\max J_{mI}(\boldsymbol{w}_{ms}, \alpha_m) = \rho log\left[\hat{p}_I \equiv \sum_q \frac{1}{2\sqrt{2\pi\rho}} exp(-\frac{(y_I - s_q)^2}{2\rho})\right],$$

subject to $\boldsymbol{w}_{msI} = -\boldsymbol{J}\boldsymbol{w}_{msI}$, (32)

where $\begin{cases} s_i \equiv \dfrac{2i - N - 1}{F} \\ s_q \equiv \dfrac{2q - N - 1}{F} \end{cases}, 1 \le i, q \le N$.

The constrained cost rules (31-32) are then transformed into unconstrained forms:

$$Q_R = J_{mR}(\boldsymbol{w}_{ms}, a_m) + \frac{\lambda_R(n)}{\| \boldsymbol{w}_{msR}(n) - \boldsymbol{J}\boldsymbol{w}_{msR}(n)\|^2}, \tag{33}$$

$$Q_I = J_{mI}(\boldsymbol{w}_{ms}, a_m) + \frac{\lambda_I(n)}{\| \boldsymbol{w}_{msI}(n) - \boldsymbol{J}\boldsymbol{w}_{msI}(n)\|^2}. \tag{34}$$

We take the gradient of (33) with respect to $\boldsymbol{w}_{msR}$ and α_{mR}, respectively, as

$$\begin{aligned} \nabla_{\boldsymbol{w}_{msR}} Q_R &= \varDelta_{mR}(n)(\alpha_{mR}(n)\boldsymbol{x}_R(n) - \alpha_{mI}(n)\boldsymbol{x}_I(n)) \\ &\quad - \frac{4\lambda_R(n)(\boldsymbol{w}_{msR}(n) - \boldsymbol{J}\boldsymbol{w}_{msR}(n))}{\| \boldsymbol{w}_{msR}(n) - \boldsymbol{J}\boldsymbol{w}_{msR}(n)\|^4}, \end{aligned} \tag{35}$$

and

$$\nabla_{\alpha_{msR}} Q_R = \varDelta_{mR}(n)\left[\boldsymbol{w}_{msR}^T(n)\boldsymbol{x}_R(n) + \boldsymbol{w}_{msI}^T(n)\boldsymbol{x}_I(n)\right], \tag{36}$$

where

$$\varDelta_{mR}(n) \equiv \frac{\sum_i \exp(\frac{(y_R(n) - s_i)^2}{2\rho})(s_i - y_R(n))}{\sum_i \exp(\frac{(y_R(n) - s_i)^2}{2\rho})}. \tag{37}$$

Similarly, we take the gradient of (34) with respect to $\boldsymbol{w}_{msI}$ and α_{mI}, respectively, as

$$\nabla_{\boldsymbol{w}_{msI}} Q_I = \Delta_{mI}(n)(\alpha_{mI}(n)\boldsymbol{x}_I(n) - \alpha_{mR}(n)x_R(n)) - \frac{4\lambda_I(n)(\boldsymbol{w}_{msI}(n) + \boldsymbol{J}\boldsymbol{w}_{msI}(n))}{\|\boldsymbol{w}_{msI}(n) + \boldsymbol{J}\boldsymbol{w}_{msI}(n)\|^4}, \quad (38)$$

and

$$\nabla_{\alpha_{msI}} Q_I = \Delta_{mI}(n)\left[\boldsymbol{w}_{msI}^T(n)\boldsymbol{x}_I(n) + \boldsymbol{w}_{msR}^T(n)\boldsymbol{x}_R(n)\right], \quad (39)$$

where

$$\Delta_{mI}(n) \equiv \frac{\sum_q \exp\left(\frac{(y_I(n)-s_q)^2}{2\rho}\right)(s_q - y_I(n))}{\sum_q \exp\left(\frac{(y_I(n)-s_q)^2}{2\rho}\right)}. \quad (40)$$

Then the updating of the weight vector $\boldsymbol{w}_{ms}$ is also separated into the real part and the imaginary part as follows:

$$\begin{aligned}\boldsymbol{w}_{msR}(n+1) &= \boldsymbol{w}_{msR}(n) \\ &+\mu_m \Delta_{mR}(n)(\alpha_{mR}(n)\boldsymbol{x}_R(n) - \alpha_{mI}(n)\boldsymbol{x}_I(n)) \\ &-\mu_m \frac{4\lambda_R(n)(\boldsymbol{w}_{msR}(n) - \boldsymbol{J}\boldsymbol{w}_{msR}(n))}{\|\boldsymbol{w}_{msR}(n) - \boldsymbol{J}\boldsymbol{w}_{msR}(n)\|^2},\end{aligned} \quad (41)$$

$$\begin{aligned}\boldsymbol{w}_{msI}(n+1) &= \boldsymbol{w}_{msI}(n) \\ &+\mu_m \Delta_{mI}(n)(\alpha_{mI}(n)\boldsymbol{x}_I(n) - \alpha_{mR}(n)\boldsymbol{x}_R(n)) \\ &-\mu_m \frac{4\lambda_I(n)(\boldsymbol{w}_{msI}(n) + \boldsymbol{J}\boldsymbol{w}_{msI}(n))}{\|\boldsymbol{w}_{msI}(n) + \boldsymbol{J}\boldsymbol{w}_{msI}(n)\|^2}.\end{aligned} \quad (42)$$

We know that $\boldsymbol{w}_{msR}(n+1)$ and $\boldsymbol{w}_{msI}(n+1)$ are constrained into the two real-valued symmetries, so we can drive the following equations:

$$\mu_m \frac{4\lambda_R(n)(\boldsymbol{w}_{msR}(n) - \boldsymbol{J}\boldsymbol{w}_{msR}(n))}{\|\boldsymbol{w}_{msR}(n) - \boldsymbol{J}\boldsymbol{w}_{msR}(n)\|^2} = \frac{\mu_m \Delta_{mR}(n)}{2}(\boldsymbol{v}_R + \boldsymbol{J}\boldsymbol{v}_R(n)), \quad (43)$$

where $\boldsymbol{v}_R(n) = (\alpha_{mR}(n)\boldsymbol{x}_R(n) - \alpha_{mI}(n)\boldsymbol{x}_I(n))$,

and

$$\mu_m \frac{4\lambda_I(n)(\boldsymbol{w}_{msI}(n) + \boldsymbol{J}\boldsymbol{w}_{msI}(n))}{\|\boldsymbol{w}_{msI}(n) + \boldsymbol{J}\boldsymbol{w}_{msI}(n)\|^2} = \frac{\mu_m \Delta_{mI}(n)}{2}(\boldsymbol{v}_I - \boldsymbol{J}\boldsymbol{v}_I(n)), \quad (44)$$

where $\boldsymbol{v}_I(n) = (\alpha_{mI}(n)\boldsymbol{x}_I(n) - \alpha_{mR}(n)\boldsymbol{x}_R(n))$. Finally, we can get the $\boldsymbol{w}_{msR}$ and $\boldsymbol{w}_{msI}$ by substituting (43) into (41) and (44) into (42):

$$\boldsymbol{w}_{msR}(n+1) = \boldsymbol{w}_{msR}(n) + \frac{\mu_m \Delta_{mR}(n)}{2}(\boldsymbol{v}_R + \boldsymbol{J}\boldsymbol{v}_R(n)), \quad (45)$$

and

$$\boldsymbol{w}_{msI}(n+1) = \boldsymbol{w}_{msI}(n) + \frac{\mu_m \Delta_{mI}(n)}{2}(\boldsymbol{v}_I - \boldsymbol{J}\boldsymbol{v}_I(n)). \quad (46)$$

We also update α_{mR} and α_{mI} in the gradient of (36) and (39) with the same stepsize μ_α and normalized it:

$$\begin{cases}\hat{\alpha}_{mR}(n+1) = \alpha_{mR}(n) + \mu_\alpha \Delta_{mR}(n)\Lambda(n) \\ \hat{\alpha}_{mI}(n+1) = \alpha_{mI}(n) + \mu_\alpha \Delta_{mI}(n)\Lambda(n)\end{cases}, \quad (47)$$

$$\alpha_m(n+1) = \frac{(\hat{\alpha}_{mR}(n+1) + j\hat{\alpha}_{mI}(n+1))}{|\hat{\alpha}_{mR}(n+1) + j\hat{\alpha}_{mI}(n+1)|}, \quad (48)$$

where $\Lambda(n) = \boldsymbol{w}_{mR}^T(n)\boldsymbol{x}_R(n) + \boldsymbol{w}_{mI}^T(n)\boldsymbol{x}_I(n)$. The blind RSC-MAP weight vector finally is expressed as $\boldsymbol{w}_m(n+1) = \alpha_m(n+1)^*(\boldsymbol{w}_{mR}(n+1) + j(\boldsymbol{w}_{mI}(n+1))$.

The RSC-MAP algorithm has guided the complex-valued-based cost rule used for SC-MAP into two real-valued-based cost rules. We will show in simulations that the CMA+RSC-MAP algorithm would obtain the same performance as the CMA+SC-MAP with less complexity.

TABLE 1
STEPSIZES WITH 4-QAM

Stepsize	CMA+ DD	CMA+ MAP	CMA+ SC-MAP	CMA+ RSC-MAP
μ_c	0.002	0.0009	0.002	0.004
μ_m	0.003	0.005	0.009	0.00001

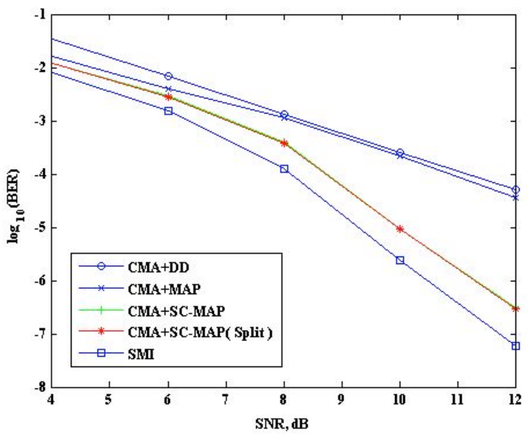

Fig. 1 BER performance at different SNRs after 600 snapshots for adapting.

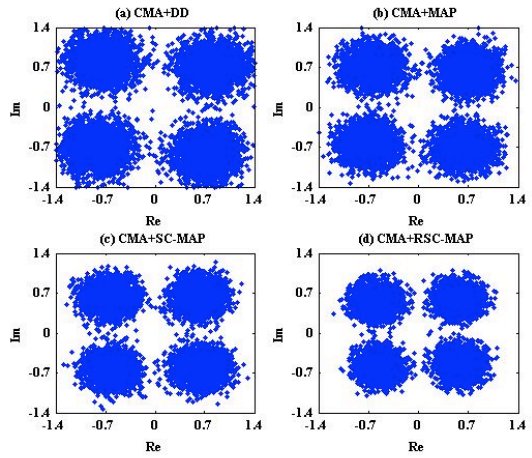

Fig. 2 Constellation of filter outputs after 600 snapshots for adapting.

4. Simulation Results

4.1 Performance Analyses

Simulations are executed to show the performance and analyses of the proposed algorithm. For all simulations, we have assumed that the linear array contains eight sensors with $d_a = \lambda_a / 2$. The blind CMA+DD [11], blind CMA+MAP [12] blind CMA+SC-MAP and optimal reference-based SMI solution with 600 reference data [2] are also simulated for purpose of comparisons.

We set four source signals arriving from the DOAs $\theta_0 = -10°$, $\theta_1 = -15°$, $\theta_2 = -30°$ and $\theta_3 = 20°$, respectively, with the first signal being the desired one. All signals have the same power and are modulated by 4-QAM. The stepsizes μ_α and μ_m for various algorithms are given in Table 1. The stepsize μ_α is set as 0.02 and 0.005 for CMA+SC-MAP and CMA+RSC-MAP, respectively. The variance ρ is set as 0.09 and 0.15 for CMA+SC-MAP and CMA+RSC-MAP, respectively. With averaging 10^5 individual runs, each run involves the adapting and testing phases obtain the results. The number of snapshots in the testing phase is 10^3.

Fig.1 shows BER curves of various algorithms after 600 snapshots for adapting. Without any available reference data, the blind CMA+RSC-MAP by 600 adaptations can be the same performance to the CMA+SC-MAP also close to the optimal reference-based SMI solutions. Apart from low SNRs, the gap as the performance in high SNRs will be more noticeably.

Fig. 2 shows constellation of filter outputs after 600 snapshots for adapting. It can be seen that the classic blind algorithms have different degrees of phase rotation. This is the major reason for the occurrence of the poor BER performance. We can see that the signals of CMA+DD, CMA+MAP and CMA+SC-MAP on the constellation are still dispersive, but the signals of the CMA+RSC-MAP algorithm on the constellation are more centralizing to the ideal 4-QAM signals than the other algorithms.

TABLE 2
Computational Complexity Per Weight Update

Algorithm	Multiplication	Division
CMA+DD	$16M+8$	N/A
CMA+MAP	$12M+5N^2+9$	2
CMA+SC-MAP	$16M+5N^2+23$	4
CMA+RSC-MAP	$15M+6N+16$	4

4.2 Complexity Analyses

The computational complexity of various CAFs is shown in Table 2. Multiplications and divisions mainly affect the computational complexity, so we only show multiplications and divisions in the table. Noting that the number N in Table II is related to probability density functions. For example, N^2-QAM requires N^2 Gaussian clusters to acquire the estimate of $\hat{p}(\boldsymbol{w}, y(n))$ for CMA+MAP and the proposed CMA+SC-MAP. When N gets higher, the multiplication will be increased by square for CMA+MAP and CMA+SC-MAP. The proposed CMA+RSC-MAP algorithm using probability density functions defined in (31-32) only requires 3N multiplications for each Gaussian clusters. Therefore, the multiplication computation of CMA+RSC-MAP could be largely saved per weight update.

5. Conclusions

In this paper, the symmetric-constrained property has been shown to be useful to derive the proposed CMA+SC-MAP and CAM+RSC-MAP algorithms. The simulations show that the

CAM+RSC-MAP obtain the same performance as the CMA+SC-MAP, and are closed to optimal reference-based SMI solutions. The phase error occurred in CMA+DD and CMA+SDD would lead to poor BER performance, but both CMA+SC-MAP and CMA+RSC-MAP do not have serious phase-error problems. Compared with the CMA+SC-MAP, the CMA+RSC-MAP greatly reduces the multiplication complexity from $16M+5N^2+23$ to $15M+6N+16$.

REFERENCES

[1] S. Haykin, *Adaptive filter theory*, 4th edition. Englewood Cliffs, NJ: Prentice-Hall, 2002.

[2] L. C. Godara, "Application of antenna arrays to mobile communications, part II: beam-forming and direction-of-arrival estimation," *Proc. IEEE*, vol. 85, pp. 1195-1245, 1997.

[3] A. I. Sulyman, and M. Hefnawi, "Adaptive MIMO beamforming algorithm based on gradient search of the channel capacity in OFDM-SDMA systems," *IEEE Commun. Lett.*, vol. 12, pp. 642-644, 2008.

[4] S. Chen, A. Livingstone, H. Q. Du, and L. Hanzo, "Adaptive minimum symbol error rate beamforming assisted detection for quadrature amplitude modulation," *IEEE Trans. Wirel. Commun.*, vol. 7, pp. 1140-1145, 2008.

[5] Y. J. Chang and C. L. Ho, "Reduced Symmetric Self-Constructing Fuzzy Neural Network Beamforming Detectors," *IET Microw. Antennas Propag.*, vol. 5, pp. 676-684, 2011.

[6] L. Zhang, W. Liu, and R. J. Langley, "A class of constrained adaptive beamforming algorithms based on uniform linear arrays," *IEEE Trans. Signal Process.*, vol. 58, pp. 3916-3922, 2010.

[7] L. Zhang, W. Liu, and R. J. Langley, "Adaptive beamforming with real-valued coefficients based on uniform linear arrays," *IEEE Trans. Antennas Propag.*, vol. 59, pp. 1047-1053, 2011.

[8] L. Wang, and R. C. de Lamare, "Constrained adaptive filtering algorithms based on conjugate gradient techniques for beamforming," *IET Signal Process.*, vol. 4, pp. 686-697, 2010.

[9] S. Chen, T. B. Cook, and L. C. Anderson, "A comparative study of two blind FIR equalizers," *Digit. Signal Prog.*, vol. 14, pp. 18-36, 2004.

[10] W. Chung, "Soft decision approaches in adaptive blind decision feedback equalizers," *Electron. Lett.*, vol. 44, pp. 1328-1329, 2008.

[11] F. D' Agostini, S. Carboni, M. C. F. De Castro, F. C. C. De Castro, and D. von B. M. Trindade, "Adaptive concurrent equalization applied to multicarrier OFDM systems," *IEEE Trans. Broadcast.*, vol. 54, pp. 441-447, 2008.

[12] S. Chen, "Low complexity concurrent constant modulus algorithm and soft decision directed scheme for blind equalization," *IEE Proc.-Vis. Image Signal Process.*, vol. 150, pp. 312-320, 2003.

[13] M. T. M. Silva, M. D. Miranda, and R. Soares, "Concurrent algorithm for blind adaptation of DFE," *Electron. Lett.*, vol. 41, pp. 63-64, 2005.

[14] B. Lin, R. He, X. Wang, and B. Wang, "Excess MSE analysis of the concurrent constant modulus algorithm and soft decision-directed scheme for blind equalization," *IET Signal Process.*, vol. 2, pp. 147-155, 2008.

[15] S. Chen and L. Hanzo, "Fast converging semi-blind space-time equalisation for dispersive QAM MIMO systems," *IEEE Trans. Wirel. Commun.*, vol. 8, pp. 3969-3974, 2009.

[16] C. P. Fan, C. H. Fang, H. J. Hu, and W. N. Hsu, "Design and analyses of a fast feed-forward blind equalizer with two-stage generalized multilevel modulus and soft decision-directed scheme for high-order QAM cable downstream receivers," *IEEE Trans. Consumer Electronics*, vol. 56, pp. 2132-2140, 2010.

[17] N. Xie, H. Hu, and H. Wang, "A new hybrid blind equalization algorithm with steady-state performance analysis," *Digit. Signal Prog.*, vol. 22, pp. 233-237, 2012.

[18] R. Mitra, S. Singh, and A. Mishra, "Improved multi-stage clustering-based blind equalization," *IET Commun.*, vol. 5, pp. 1255-1261, 2011.